

Enhancement of the c_{11} Elastic Constant of Ag/Pd Superlattice Films as Determined from Longitudinal Guided Modes

John R. Dutcher, Sukmock Lee, Jeha Kim, George I. Stegeman, and Charles M. Falco
Optical Sciences Center and Department of Physics, University of Arizona, Tucson, Arizona 85721
 (Received 11 June 1990)

In Brillouin-light-scattering studies of a series of Ag/Pd superlattice films we have observed scattering from longitudinal guided modes (LGMs) whose velocities are determined primarily by the c_{11} elastic constant. From the measured velocity of the first-order LGM, we have obtained the first accurate determination of c_{11} for metallic thin films. For the Ag/Pd superlattice films, large increases in both the longitudinal (c_{11}) and shear (c_{55}) elastic constants were observed as the superlattice modulation wavelength Λ was decreased below $\Lambda = 60 \text{ \AA}$.

PACS numbers: 62.20.Dc, 62.30.+d, 68.60.Bs, 78.35.+c

The elastic properties of metallic superlattice films have been shown to depend on the superlattice modulation wavelength Λ .¹⁻⁹ Dramatic enhancements of up to 500% in the biaxial modulus Y_B for $\Lambda \approx 25 \text{ \AA}$ were inferred from bulge tester measurements.^{1,2} More recently, Brillouin light scattering (BLS) has been used to study metallic superlattice films.³⁻⁸ Changes of up to 20% in the Rayleigh mode velocity have been observed^{3,8} as Λ was varied between 5 and 100 \AA .

The elastic constants of metallic films can be determined from BLS measurements of the Rayleigh and Sezawa⁴⁻⁶ film-guided acoustic-mode velocity dispersion. For sputtered films which have hexagonal symmetry,⁸ the velocities of these modes are determined by four of the five independent elastic constants: c_{11} , c_{13} , c_{33} , and $c_{55} = c_{44}$. For film thicknesses greater than 3000 \AA , the Rayleigh mode velocity is determined almost entirely by c_{55} .⁸ However, it is very difficult to distinguish the contributions of the other three elastic constants to the Sezawa mode velocities.^{4-6,10} Because of this, in previous BLS studies,⁴⁻⁶ two elastic constants were fixed to their average values and the remaining two elastic constants were obtained by using a least-squares-fitting procedure. Despite combining such fits to the measured mode velocities with comparisons of the measured and calculated scattering intensities, ambiguities in the elastic constant values were obtained.¹⁰

In the present work, we report the first identification of light scattering from the longitudinal guided modes (LGMs) of metallic films. LGMs are film-guided acoustic modes which have displacements primarily along the propagation direction in the film plane, and velocities that are strongly dependent on the longitudinal elastic constant c_{11} . In previous BLS studies,^{11,12} LGMs were observed for films that were transparent to the light. For transparent films, strong LGM peaks are observed in the BLS spectra since the large penetration depth of the light δ_{opt} produces a large amount of elasto-optic scattering.¹³ However, for metallic films, δ_{opt} ($\approx 150 \text{ \AA}$) is much smaller than for transparent films, so that the

scattering intensity is due almost entirely to the surface ripple mechanism.¹³ For semi-infinite metallic films, the LGMs become the longitudinal resonance,¹⁴ there is no surface ripple, and a dip corresponding to the longitudinal resonance should be observed in BLS spectra.¹⁴ However, for films of finite thickness, such as the Ag/Pd superlattice films described below, there is a small amount of surface ripple scattering which produces weak, but measurable, peaks in the BLS spectra corresponding to the LGMs.

Using the first-order-LGM measured velocity, we have developed a procedure to obtain the first accurate determination of c_{11} for thin metallic films. We have used this procedure to measure the Λ dependence of c_{11} for a series of Ag/Pd superlattice films. The Ag/Pd superlattice system is particularly interesting since a 500% enhancement in Y_B has been reported for this system.² For sputtered metallic films which have hexagonal symmetry,⁸ $Y_B = c_{11} + c_{12} - 2(c_{13}^2/c_{33})$, where $c_{11} \approx c_{33} \approx 2c_{12} \approx 2c_{13}$. Because c_{11} is the largest contribution to Y_B , the accurate determination of c_{11} for metallic superlattice films is an important step toward the reconciliation of BLS and bulge tester measurements of these films.

The BLS results presented below were obtained from a series of fifteen Ag/Pd superlattice films that were grown using magnetically enhanced dc triode sputtering techniques.¹⁵ These films were designed to have 51 at. % Ag, modulation wavelength Λ values between 5 and 110 \AA , and total film thicknesses $h \approx 4500 \text{ \AA}$. Details of the structural characterization of the films using high- and low-angle x-ray diffraction, and Rutherford backscattering, will be given elsewhere.¹⁵ In the BLS experiments, typically 100 mW of laser light ($\lambda = 5145 \text{ \AA}$), polarized in the plane of incidence, was focused onto the sample surface. Diffusely scattered light was collected using a 180° backscattering geometry, and frequency analyzed using a high-contrast, tandem (3+3 passes) Sandercock-type Fabry-Pérot interferometer.¹³

A BLS spectrum for a Ag/Pd superlattice film with

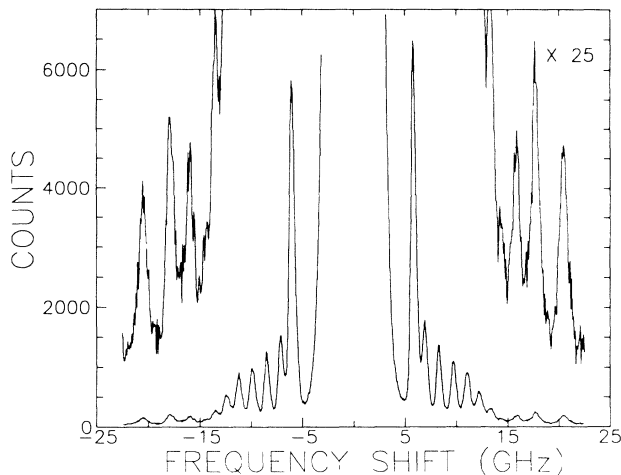


FIG. 1. Brillouin-light-scattering spectrum for a Ag/Pd superlattice film with 51 at. % Ag, modulation wavelength $\Lambda=37$ Å, and total thickness $h=4570$ Å. The angle of incidence was $\theta=70^\circ$, the incident laser power was 100 mW, and the total data collection time was 16.5 h.

$\Lambda=37$ Å and total film thickness $h=4570$ Å is shown in Fig. 1. The peaks with frequency shifts between 6 and 14 GHz are due to light scattering from the Rayleigh and Sezawa modes. Also, there are three weak peaks between 16 and 21 GHz which are shown with an expanded vertical scale as an inset to Fig. 1. All of the peaks in the spectrum have narrow linewidths which are determined by the Fabry-Pérot interferometer instrumental function.

Velocity dispersion curves for the $\Lambda=37$ Å Ag/Pd sample are shown in Fig. 2. The solid curves were calculated using the procedure of Farnell and Adler¹⁶ and the best-fit elastic-constant values. The agreement between the data and the calculated curves is excellent. In addition to the branches of data corresponding to the Rayleigh and Sezawa modes, there are also branches of data with velocities $v > 4000$ m/s corresponding to the weak peaks in Fig. 1. To understand the origin of these weak peaks, the range of qh values for the calculated velocity dispersion curves has been extended to $qh=20$. For $v > 4000$ m/s, the calculated curves are quite complicated since they consist of two different sets of curves. One set corresponds to the Sezawa modes, whose asymptotic velocity value for large qh is close to the Rayleigh mode velocity $v_R=1620$ m/s. The second set corresponds to an additional set of high-velocity modes, whose asymptotic velocity value for large qh agrees closely (within 1.3% for $qh=20$) with the film longitudinal velocity $v_L=\sqrt{c_{11}/\rho}=4140$ m/s. These two sets of curves do not intersect. Instead, the modes hybridize near the crossing points, forming gaps in the dispersion curves. Because of the close correspondence between v_L and the asymptotic velocity value of the set of high-velocity modes, we have identified these modes as the longitudinal guided

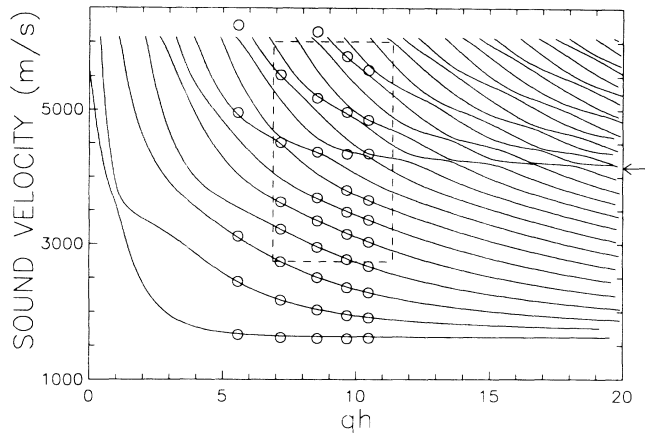


FIG. 2. Velocity dispersion curves for the $\Lambda=37$ Å Ag/Pd sample, for which q is the in-plane wave-vector component and h is the total film thickness. The open circles are data and the solid curves were calculated using the best-fit film elastic constants (in GPa) $c_{11}=193$, $c_{13}=119$, $c_{33}=195$, and $c_{55}=32.3$; film density $\rho=11.23$ g/cm³; elastic constants of sapphire substrate (in GPa) $c_{11}=497$, $c_{12}=203$, and $c_{55}=147$; and sapphire density $\rho_s=3.986$ g/cm³. The horizontal arrow indicates the film longitudinal velocity $v_L=4140$ m/s.

modes^{11,12} of the film. The weak peaks in Fig. 1 correspond to light scattering from the three lowest-order (lowest-velocity) LGMs.

Figure 3 shows a three-dimensional version of the velocity dispersion curves, in which the scattering intensity is plotted versus both sound velocity and qh . This plot corresponds to the small area of the two-dimensional dispersion curves contained within the dashed lines in Fig. 2. In the three-dimensional plot, the intensities were calculated using the procedure of Bortolani *et al.*¹⁷ and include only the surface-ripple contribution. It can be seen that the peaks in the scattering intensity follow the dispersion of the LGMs and not that of the Sezawa modes. The intensities of the LGM peaks are small. For comparison, for the $\Lambda=37$ Å Ag/Pd sample and $qh=10.3$, the scattering intensity of the first-order LGM is only 1.9% that of the Rayleigh mode, in both calculation and experiment.

To verify the assignment of the set of high-velocity modes in Figs. 2 and 3 as the LGMs of the film, we have performed two different calculations. The LGM velocities v_{LGM} should depend strongly on c_{11} . Because of this, for the mode which we have identified as the first-order LGM, we have calculated the dependence of the elastic constant $c_{LGM}=\rho(v_{LGM})^2$ on each of the independent elastic constants while fixing the other elastic constants at their equilibrium values. For the $\Lambda=37$ Å Ag/Pd sample and $qh=10.3$, c_{11} has the largest effect on c_{LGM} : a +15% (−15%) change in c_{11} produces a change in c_{LGM} of +12.0% (−11.5%), respectively. This strong dependence of c_{LGM} on c_{11} is very similar to the depen-

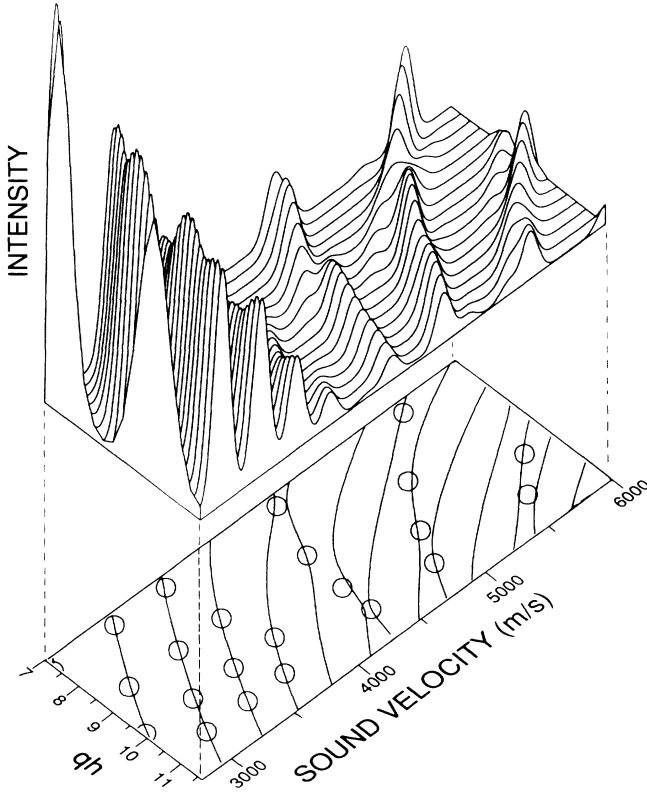


FIG. 3. Calculated three-dimensional velocity dispersion curves in which the scattering intensity is plotted vs sound velocity and qh for the $\Lambda=37$ Å Ag/Pd sample. The two-dimensional dispersion curves, which correspond to the rectangular area enclosed by dashed lines in Fig. 2, is shown at the bottom.

dence of the Rayleigh mode modulus c_R on c_{55} .⁸ The dependence of c_{LGM} on the other elastic constants is much weaker: Changes of +15% (–15%) in c_{13} , c_{33} , and c_{55} produce changes in c_{LGM} of only +0.5, +2.1, and +2.1% (+2.9, –0.9, and –1.6%), respectively.

Second, LGMs are predominantly longitudinally polarized, so that the displacement component u_{\parallel} parallel to the film surface should be much larger than the perpendicular component u_{\perp} . We have calculated $|u_{\parallel}|^2$ and $|u_{\perp}|^2$ across the thickness of the film for the first-order LGM of the $\Lambda=37$ Å Ag/Pd sample with $qh=10.3$, and we find that the predominantly longitudinal displacement profiles for this mode are very similar to those for LGMs observed in transparent materials.^{11,12} The peak value of $|u_{\parallel}|^2$ exceeds the peak value of $|u_{\perp}|^2$ by a factor of 8. Thus, both the strong dependence of c_{LGM} on c_{11} and the large degree of longitudinal polarization for the first-order LGM confirm our assignment of the high-velocity modes in Figs. 2 and 3 as the LGMs of the film.

We have developed a procedure to determine c_{11} for a metallic film using the first-order LGM velocity. First, the intensity spectrum is calculated using an initial set of elastic constants and the qh value corresponding to the

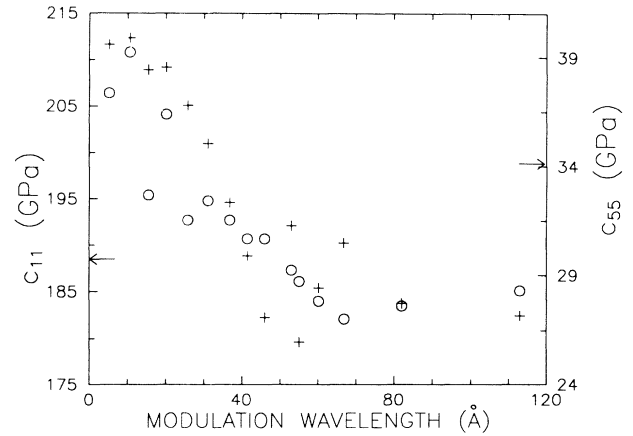


FIG. 4. The measured Λ dependence of the c_{11} (O) and c_{55} (+) elastic constants for a series of fifteen Ag/Pd superlattice films. The horizontal arrows indicate the elastic constants calculated using the procedure of Grimsditch (Ref. 18) for a “bulk” Ag/Pd superlattice film, consisting of Ag and Pd layers with bulk elastic constants and 51 at. % Ag (Ref. 8).

experimental scattering geometry. The LGM peaks in this spectrum are then identified from the calculated displacement profiles and the LGM velocity v_{LGM}^{calc} is used to calculate the ratio R between the input value of c_{11} and the elastic constant $c_{LGM} = \rho(v_{LGM}^{calc})^2$. R is typically 0.9 for $qh=10$. This value of R is then used together with the experimental LGM velocity v_{LGM}^{expt} to calculate a new value of $c_{11} = R[\rho(v_{LGM}^{expt})^2]$. Using this new value of c_{11} , a least-squares fit to the BLS data is performed to obtain c_{13} , c_{33} , and c_{55} . Finally, this new set of elastic constants is used to obtain a new value of R . This procedure is iterated until the values of R on two successive iterations differ by less than a few percent.

The Λ dependence of c_{11} and c_{55} for a series of Ag/Pd superlattice films is shown in Fig. 4. The values of c_{11} were determined using the procedure described above. This procedure converges rapidly: After only one iteration, the values of the ratio R for the entire series of films were within 1.5% of the original value $R=0.908$ that was computed for the “bulk” Ag/Pd superlattice film described in the caption of Fig. 4. It can be seen that c_{11} increases monotonically as Λ decreases below 60 to 5 Å. The total increase in c_{11} is 14%. The values of c_{55} were obtained from a least-squares fit of the BLS data although, as mentioned above, c_{55} is determined primarily by the Rayleigh mode velocity. The values of c_{55} also increase monotonically as Λ decreases. The total change in c_{55} is 50%, which is the largest change observed to date for any metallic superlattice system. It is possible that this monotonic behavior of c_{11} and c_{55} is due to the presence of stiff interfaces between the Ag and Pd layers, since the interface contribution to the elastic constants becomes increasingly more important as Λ is decreased. Unlike the Y_B data reported for Ag/Pd films,² there is no feature in either the c_{11} or c_{55} data

near $\Lambda = 25 \text{ \AA}$. Ag/Pd is also the first metallic superlattice system for which both the longitudinal (c_{11}) and shear (c_{55}) elastic constants have the same qualitative Λ dependence. Not only do both c_{11} and c_{55} increase with decreasing Λ , but for $\Lambda \leq 30 \text{ \AA}$, the films are stiffer than the "bulk" Ag/Pd superlattice film. The full details of the elastic properties of the Ag/Pd films will be presented elsewhere.¹⁵

In summary, we have observed weak light scattering from a set of high-velocity modes of metallic superlattice films, which we have identified as the longitudinal guided modes. We have used the measured velocity of the first-order LGM to obtain the first accurate determination of the c_{11} elastic constant of a thin metallic film. For Ag/Pd superlattices we have observed large increases in both c_{11} and c_{55} as Λ was decreased. This is the first metallic superlattice system studied thus far for which both c_{11} and c_{55} have the same qualitative Λ dependence.

We thank Professor F. Nizzoli and Dr. B. Hillebrands for the use of their computer programs. J.R.D. is grateful to the Natural Sciences and Engineering Research Council of Canada for a postdoctoral fellowship. This work was supported by the Office of Naval Research under Contract No. N00014-88-K-0298.

¹W. M. C. Yang, T. Tsakalakos, and J. E. Hilliard, *J. Appl. Phys.* **48**, 876 (1977).

²G. E. Henein and J. E. Hilliard, *J. Appl. Phys.* **54**, 728 (1983).

³A. Kueny, M. Grimsditch, K. Miyano, I. Banerjee, C. M.

Falco, and I. K. Schuller, *Phys. Rev. Lett.* **48**, 166 (1982).

⁴P. Baumgart, B. Hillebrands, R. Mock, G. Güntherodt, A. Boufelfel, and C. M. Falco, *Phys. Rev. B* **34**, 9004 (1986).

⁵J. A. Bell, W. R. Bennett, R. Zanoni, G. I. Stegeman, C. M. Falco, and F. Nizzoli, *Phys. Rev. B* **35**, 4127 (1987).

⁶J. A. Bell, W. R. Bennett, R. Zanoni, G. I. Stegeman, C. M. Falco, and C. T. Seaton, *Solid State Commun.* **64**, 1339 (1987).

⁷M. Grimsditch, in *Light Scattering in Solids V*, edited by M. Cardona and G. Güntherodt (Springer-Verlag, Berlin, 1989), p. 284.

⁸J. R. Dutcher, S. Lee, C. D. England, G. I. Stegeman, and C. M. Falco, *J. Mater. Sci. Eng. B* **6**, 199 (1990).

⁹B. Clemens and G. L. Eesley, *Phys. Rev. Lett.* **61**, 2356 (1988).

¹⁰F. Nizzoli, R. Bhadra, O. F. de Lima, M. B. Brodsky, and M. Grimsditch, *Phys. Rev. B* **37**, 1007 (1988).

¹¹B. Hillebrands, S. Lee, G. I. Stegeman, H. Cheng, J. E. Potts, and F. Nizzoli, *Phys. Rev. Lett.* **60**, 832 (1988).

¹²F. Nizzoli, B. Hillebrands, S. Lee, G. I. Stegeman, G. Duda, G. Wegner, and W. Knoll, *Phys. Rev. B* **40**, 3323 (1989).

¹³J. R. Sandercock, in *Light Scattering in Solids III*, edited by M. Cardona and G. Güntherodt (Springer-Verlag, Berlin, 1982), p. 173.

¹⁴R. E. Camley and F. Nizzoli, *J. Phys. C* **18**, 4795 (1985).

¹⁵J. R. Dutcher, S. Lee, J. Kim, G. I. Stegeman, and C. M. Falco (to be published).

¹⁶G. W. Farnell and E. L. Adler, in *Physical Acoustics*, edited by W. P. Mason and R. N. Thurston (Academic, New York, 1972), Vol. IX, Chap. 2.

¹⁷V. Bortolani, A. M. Marvin, F. Nizzoli, and G. Santoro, *J. Phys. C* **16**, 1757 (1983).

¹⁸M. Grimsditch, *Phys. Rev. B* **31**, 6818 (1985).